Efficient Light-Emitting Electrochemical Cells (LECs) Based on Ionic Iridium(III) Complexes with 1,3,4-Oxadiazole Ligands

*Jing Zhang, Li Zhou, Hameed A. Al-Attar, Kuizhan Shao, Li Wang, Dongxia Zhu,*Zhongmin Su,* Martin R. Bryce,* and Andrew P. Monkman*

Eight new iridium(III) complexes 1-8, with 1,3,4-oxadiazole (OXD) derivatives as the cyclometalated C^N ligand and/or the ancillary N^N ligands are synthesized and their electrochemical, photophysical, and solid-state light-emitting electrochemical cell (LEC) properties are investigated. Complexes 1, 2, 7 and 8 are additionally characterized by single crystal X-ray diffraction. LECs based on complexes 1-8 are fabricated with a structure indium tin oxide (ITO)/poly(3,4-ethylenedioxythiophene):poly(styrenesulfonate) (PEDOT:PSS)/ cationic iridium complex:ionic liquid/Al. LECs of complexes 1–6 with OXD derivatives as the cyclometalated ligands and as the ancillary ligand show yellow luminescence (λ_{max} = 552–564 nm). LECs of complexes 7 and 8 with cyclometalated C^N phenylpyridine ligands and an ancillary N^N OXD ligand show red emission (λ_{max} 616–624 nm). Using complex 7 external quantum efficiency (EQE) values of >10% are obtained for devices (210 nm emission layer) at 3.5 V. For thinner devices (70 nm) high brightness is achieved: red emission for 7 (8528 cd m^{-2} at 10 V) and yellow emission for 1 (3125 cd m^{-2} at 14 V).

1. Introduction

Solid-state light-emitting electrochemical cells (LECs) have attracted a great deal of interest in the past few years.[1–3] Compared with conventional organic light-emitting diodes (OLEDs) with multilayer structures and low-work-function cathodes to achieve high efficiencies and low operating voltages, LECs generally comprise only one light-emitting layer, which can be easily processed from solutions, and they can use air-stable cathodes such as aluminum.

The first solid-state LEC device was based on a polymer blend containing a light-emitting polymer, an ion-conducting polymer and an inorganic salt.[4] Since the report of LECs based on an ionic transition metal complex (iTMC) in 1996 by Rubner et al.,[5] iTMC-based LECs have received ever increasing attention because they have several advantages over conventional polymer-based LECs.[1,2,6–19] In iTMC-based LECs no ion-conducting material or inorganic salt are needed because the metal complexes are intrinsically ionic. Moreover, they show good thermal and photophysical stabilities, and high electroluminescence (EL) efficiencies are achieved because of the phosphorescent nature of the metal complexes. Many efforts have been made to improve the performance of LECs. A range of iTMCs based on iridium,[10,11,20–33] ruthenium,[7b,7h,7j,7p,34,35] osmium,[8b] platinum,[36,37] and copper[9a,9c,9d] have been used to fabricate LECs, and high efficiency and brightness have been achieved. However, as a result of the higher ligand-field spitting energy of the trivalent iridium ion,[2,13–19] higher luminescent efficiency and stability,[11] and tunable emission color,[2,12–14,16–18]a,[29,30,32,39] ionic iridium complexes are the most widely researched. Efficient green,[16,18,38,42] yellow,[17,41] orange,[18,28,31] and red[13,40] LECs based on cationic iridium complexes, have been achieved. The main requirements for iTMC-LECs are that the phosphorescent emitter should have sharp colors in the red, green, and blue regions and exhibit very high phosphorescence quantum yields.

1,3,4-Oxadiazole (OXD) derivatives have high electron affinities, which make them good candidates for electron injection and transport,[43] high photoluminescence quantum yield, and good thermal and chemical stabilities; these features have led to their extensive applications in O/PLEDs,[43–45] and they have been applied in a few cases as cyclometalated ligands to enhance the optoelectronic properties of iridium complexes.[46] However, to the best of our knowledge, OXD derivatives have

J. Zhang, L. Zhou, Dr. K. Shao, L. Wang, Dr. D. Zhu, Prof. Z. Su
Institute of Functional Material Chemistry
Faculty of Chemistry
Northeast Normal University
Renmin Road 5268, Changchun, Jilin 130024 P. R. China
E-mail: zhudx047@nenu.edu.cn; zmsu@nenu.edu.cn
Dr. H. A. Al-Attar, Prof. A. P. Monkman
Department of Physics
Durham University
Durham, DH1 3LE, UK
Prof. M. R. Bryce
Department of Chemistry
Durham University
Durham, DH1 3LE, UK
E-mail: m.r.bryce@durham.ac.uk

DOI: 10.1002/adfm.201300344

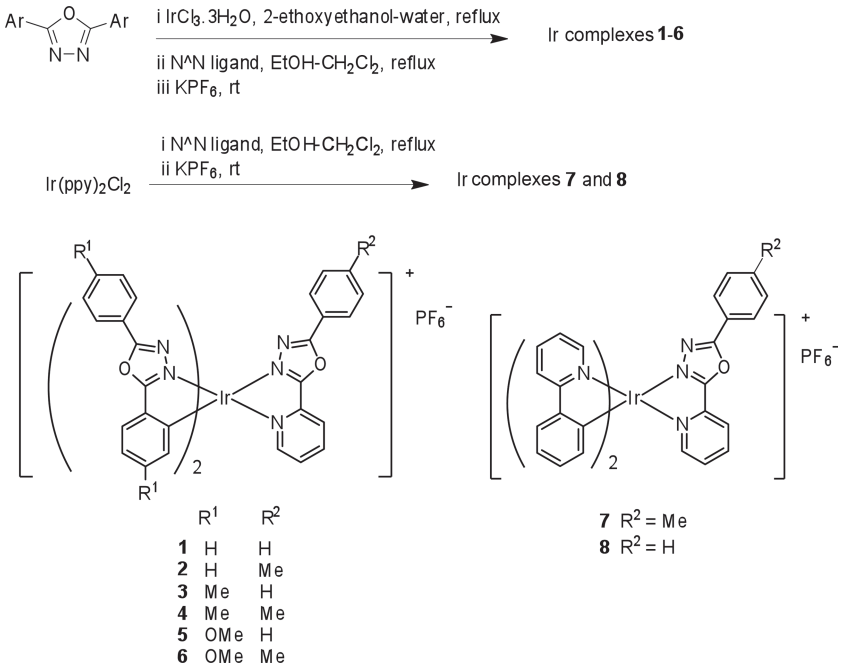

Scheme 1. Synthesis of the Ir complexes **1-8** used in this study.

not previously been reported as ligands in iTMCs for use in LECs.

Based on the above considerations, we now report the synthesis and optoelectronic characterization of eight new ionic iridium(III) complexes **1-8** (**Scheme 1**). The new molecular design feature in this work is the use of OXD ligands: these are cyclometalating C^N derivatives of 2,5-diphenyl-1,3,4-oxadiazole, and N^N coordinating 2-phenyl-5-(2-pyridyl)-1,3,4-oxadiazole derivatives. We report the structure-property relationships of the electrochemical, photophysical and electroluminescent characteristics within this series of complexes, with emphasis on tuning the color of the luminescence and the efficiency of the LECs.

2. Results and Discussion

2.1. Preparation and Characterization

The OXD ligands were synthesized in high yields from their hydrazide precursors (see Supporting Information). Scheme 1 shows a general route used to prepare the cationic iridium complexes **1-8**. Following established literature procedures for analogues,[48] in the first step, $IrCl_3 \cdot 3H_2O$ reacted with an excess of the cyclometalating ligands (3×) to give the intermediate bis(μ-Cl) bridged dimer complex, which was then reacted with the ancillary N^N ligand to afford the cationic iridium complexes in high yields. The final step was counter-ion exchange reaction from Cl^- to PF_6^- to give complexes **1-8**. All of the complexes were characterized by ^1H NMR spectroscopy, mass spectrometry and elemental analysis.

To further confirm the molecular structures of complexes **1**, **2**, **7** and **8** single crystals were characterized by X-ray crystallography. The molecular structures of **1** and **7** are shown in **Figure 1**, 2 and 8 are shown in Figure S1 in the Supporting Information. Complexes **1**, **2**, **7** and **8** all have distorted octahedral geometry around the iridium center which is coordinated by two cyclometalated ligands (C^N) and one ancillary ligand (N^N), adopting C,C-*cis* and N,N-*trans* configurations, as previously reported for cationic iridium complexes.[13a,14b,17b,30] Take complex **1** for example: the Ir-N bond distances between the Ir center and the 2-(5-phenyl-1,3,4-oxadiazol-2-yl)pyridine (pop) ancillary ligand, Ir(1)-N(1) (2.142 ± 0.010) Å and Ir(1)-N(2) 2.127 Å ± 0.009 Å are longer than those between the Ir center and the 2,5-diphenyl-1,3,4-oxadiazole (OXD) cyclometalated ligands, Ir(1)-N(4) 2.022 Å ± 0.010 Å and Ir (1)-N(6) 2.013 Å ± 0.009 Å. This trend is also observed in the structures of complexes **2**, **7** and **8** and is attributed to the stronger interaction between the anionic nature of the cyclometalated ligands and the cationic Ir(III) ion.[18] A pattern of weak interactions can be detected: face-to-face π-stacking interactions occur between the pyridyl rings in the adjacent ancillary ligands in the crystal structure of **7**. Similar π-stacking interactions between the pyridyl and phenyl rings can be seen in the crystal structure of **8**. The intermolecular π–π distances are 3.62 Å for **7** and 3.55 Å for **8**, respectively (Supporting Information Figure S2). However, there are no such interactions in the crystal structures of **1** and **2**.

The complexes are soluble in acetonitrile or dichloromethane solutions from which thin films were spin-coated. Atomic force microscopy (AFM) measurements on thin films on indium tin oxide (ITO)/poly(3,4-ethylenedioxythiophene):poly(styrenesulfonate) (PEDOT:PSS) substrates were conducted to assess the effect of adding the ionic liquid $BMIMPF_6$ to the complexes. The images established that films of uniform morphology were readily obtained with no particular aggregation or phase

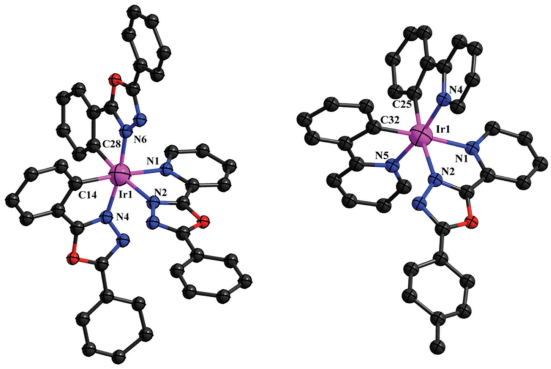

Figure 1. The cation in the molecular structure of complexes **1** (left) and **7** (right) in the crystal. The H atoms, PF_6^- anions and solvent molecules are omitted for clarity.

Table 1. Photophysical properties of complexes **1-8**.

Complex	$\lambda_{max,abs}$ [nm] solution [a]	Peak molar absorption (ε) $\times 10^4$ [$M^{-1}cm^{-1}$][a]	$\lambda_{max,em}$ [nm] solution[a]	film[b]	Φ_{PL} [%] solution[c]	Φ_{PL} [%] Film	Lifetime τ [µs] solution[f]	film [g]	k_r [s^{-1}][h]	k_{nr} [s^{-1}]
1	275, 306, 370	4.80, 3.50, 1.15	550	569	22.9		10[d]	0.524 (17%) 3.15 (83%)	1.09×10^6	3.67×10^6
2	275, 308, 331, 370	3.17, 2.47, 1.56, 0.72	534	546	30.9	8.9[d]	0.680	0.956 (27%) 3.81 (73%)	4.54×10^5	1.01×10^6
3	278, 313, 330, 374	6.20, 3.92, 3.14, 1.70	551	568	24.3	10[d]	0.460	0.970 (27.5%) 3.84 (72.5%)	5.28×10^5	1.64×10^6
4	278, 306, 329, 370	3.07, 2.51, 1.60, 0.78	546	556	13.9	3.2[d]	0.476	0.969 (27.4%) 3.83 (72.6%)	2.92×10^5	1.80×10^6
5	273, 308, 332, 370	3.70, 3.40, 2.86, 1.72	556	567	35.1	5.1[d]	0.377	0.888 (35%) 3.28 (65%)	9.31×10^5	1.72×10^6
6	370, 307, 333, 372	3.43, 3.50, 2.93, 1.67	552	558	37.0	6.4[d]	0.429	1.75 (57.7%) 5.14 (42.3%)	8.62×10^5	1.46×10^6
7	259, 296, 378	5.90, 4.38, 1.02	573	625	58.2	20[e]	0.219	0.277	2.66×10^6	1.90×10^6
8	258, 282, 378	5.40, 4.53, 1.02	556	627	24.3	17.8[e]	0.220	0.433	1.10×10^6	3.44×10^6

[a]In dichloromethane solution (1×10^{-5} M); [b]Thin film spin-coated from dichloromethane solution; [c]Photoluminescence quantum yield (PLQY) in degassed dichloromethane (error: ±5%); [d]PLQY in thin film, spin-coated from MeCN solution (error: ±5%); [e]PLQY doped in zeonex at 20% concentration (error: ±5%); [f]Lifetime data in dichloromethane solution: excitation wavelength 284 nm; [g]The figures in parentheses denote the percentage of each lifetime component; [h]k_r and k_{nr} in solution were calculated according to the equations: $k_r = \Phi/\tau$ and $k_{nr} = (1 - \Phi)/\tau$.

separation features. Representative images for complex **7** are shown in Supporting Information Figure S3.

2.2. Photophysical Properties

The photophysical data are collated in **Table 1**. **Figure 2** shows the absorption and photoluminescence spectra of the complexes in dilute CH_2Cl_2 solution. The intense absorption bands in the ultraviolet region ranging between 250 nm and ≈350 nm are assigned to the spin-allowed the ligand centered (LC) transitions. These LC bands are accompanied by weaker and broad absorption bands extending from 350 nm to the visible region, which are primarily due to the spin-allowed metal-to-ligand-charge-transfer (^{1}MLCT) transitions, ^{1}LLCT (ligand-to-ligand charge-transfer), ^{3}MLCT, ^{3}LLCT, and ligand-centered (LC) $^3\pi$–π* transitions.[47] The quantum chemical calculations (Section 2.4) are consistent with the photophysical observations. As the presence of the heavy iridium center results in a strong spin-orbit coupling, these singlet to triplet transitions become partially allowed and gain considerable intensity by mixing with the ^{1}MLCT transitions.[49]

Upon excitation all of the complexes show yellow to orange emission (534–573 nm) in degassed CH_2Cl_2 solutions with photoluminescence quantum yields (PLQYs) (Φ_{PL} = 14-58%); in thin films the quantum yields are significantly lower (Φ_{PL} = 3-20%) for all complexes except **8**, for which the solution and film yields are reproducibly quite similar. This could arise due to the film morphology leading to less concentration quenching for **8**. As shown in Figure 2 and Table 1, the λ_{max} wavelengths of complexes **1-6** are all rather similar with no particular trends and are in the range 534–556 nm in dichloromethane solution and 546–569 nm in thin film, observed as bright yellow emission. For the analogous phenylpyridinato complexes **7** and **8** the λ_{max} values are significantly red shifted to 556–573 nm (solution) and 625–627 nm (thin film), observed as bright red emission. The difference in emission color among them indicates that the introduction of the electron-withdrawing cyclometalated ligands (OXD) to **1-6** has a strong effect on the energy levels of these complexes.[17b,18] Furthermore, the ppy cyclometatalated ligands in **7** and **8** are smaller than the OXD cyclometalated ligands in **1-6**. We also compared the different packing modes in the crystal structure of the complexes. We note that enhanced π–π intermolecular interactions exist in the crystal structures of **7** and **8** (Supporting Information Figure S2), whereas no such interactions were detected in the crystal structures of **1** and **2**. This interaction could also contribute to the red shift observed for **7** and **8** due to excimer emission, as observed previously.[37] The unstructured shape of the emission bands of all the complexes **1-8** is typical of pronounced metal-to-ligand charge transfer (^{3}MLCT) electronic transitions.[40] The long tails extending to ca. 700 nm (for **1-6**) and ca. 800 nm (for **7** and **8**) in the PL spectra

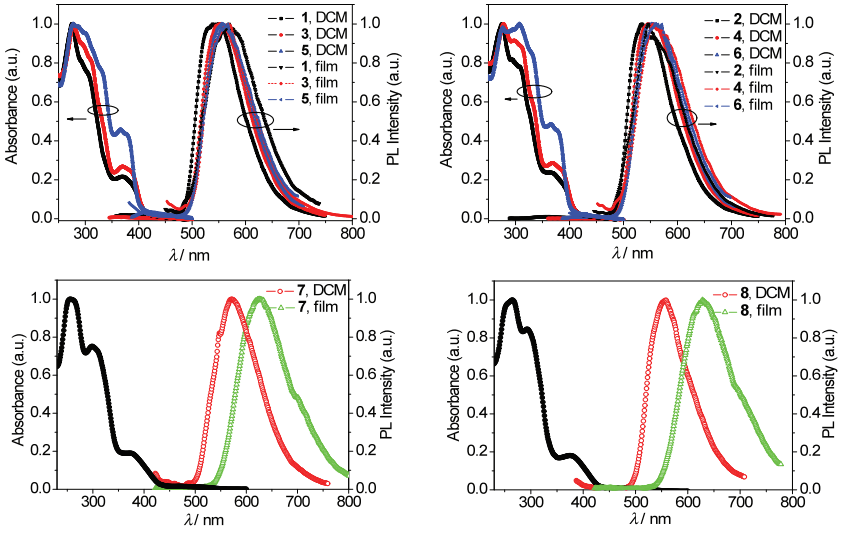

Figure 2. Normalized absorption and emission spectra of complexes **1-8** in degassed CH_2Cl_2 solutions and neat thin films at room temperature.

in thin films are consistent with strong intermolecular interactions, which could also account for the lower quantum yields in thin film compared to solution.[35] These conclusions are supported by the observation that the emission of the unsubstituted $[Ir(ppy)_2(bpy)]^+(PF_6^-)$ exhibits emission shifts of 80 nm from solid-state to solution.[17b,18]

Table 1 gives the excited-state lifetimes of complexes **1-8** in degassed CH_3CN solutions. The relatively long PL decay lifetimes–on the order of microseconds–are consistent with emissive excited states that are a mixture of LC $^3\pi$–π^* and ^{3}MLCT character.[18b,40] From the quantum yields Φ and the lifetime τ values, the radiative and non radiative decay rates k_r and k_{nr} were calculated using the equations $k_r = \Phi/\tau$ and $k_{nr} = (1 - \Phi)/\tau$.[52] Their radiative decay rates (k_r) are in the range 2.92×10^5–2.66×10^6 s^{-1}, whereas their nonradiative decay rates (k_{nr}) are longer (1.01×10^6–3.44×10^6 s^{-1}). These higher values of complex **1** are supported by the shorter emission lifetimes both in solution and film of **1** with respect to those of complexes **2-6**.[13a,52] The higher k_{nr} value of complex **1** is probably correlated with the different substituents on the OXD ligands, which might control the nonradiative pathway of decay.[52] The higher quantum yields of **7** and **8** (especially in thin films) can be attributed to their increased radiative rates which are significantly greater than those of **1-6**. These data indicate that the substituents can change the photophysical properties of the iridium complexes without modifying the nature of the emitting triplet state. The knowledge of these photophysical parameters assists in evaluating the potential applications of these complexes in LEC devices.

2.3. Electrochemical Properties

The solution electrochemical properties of the complexes were determined by cyclic voltammetry (CV). **Figure 3** shows the CVs of **1-8** and the measured redox potentials are listed in **Table 2**. As shown in Figure 3, all of the complexes exhibit quasi-reversible reduction processes and irreversible oxidation processes in CH_3CN solutions. The oxidation (E_{ox}) and reduction potentials (E_{red}) are obtained from the anodic (E_{pa}) and cathodic (E_{pc}) peak potentials.

The electronic structure calculations (Section 2.4) establish that the highest occupied molecular orbital (HOMO) is located on a mixture of the d orbitals of iridium and the π orbitals of the phenyl ring of the cyclometalated ligand, and the lowest unoccupied molecular orbital (LUMO) is located mainly on the ancillary N^N ligand, as usual for $(C^N)_2Ir(N^N)$ complexes.[2a,3a,7q] Consequently, the oxidation processes occur with metal-centered orbitals and a contribution from the phenyl ring of the cyclometalated fragments (OXD or ppy), whereas the reduction processes involve the orbitals centered on the Ir-ancillary N^N ligand.[52b] Only small effects on the redox potentials (±10–20 mV) are observed within the series **1-6** with varying H, Me or OMe substituents. It is interesting that the electronic nature of the cyclometalated ligand exerts a subtle effect on the reduction potential.[35c] The higher reduction of complex **2**, which also contains the same ancillary ligand as **7**, is likely to be associated with the more electron-withdrawing OXD cyclometalated ligands in complex **2**. It can be seen that the energies of the frontier orbitals in these complexes can be subtly manipulated by tailoring the electronic properties of the cyclometalated ligands. For example, the LUMO for **2** is destabilized compared

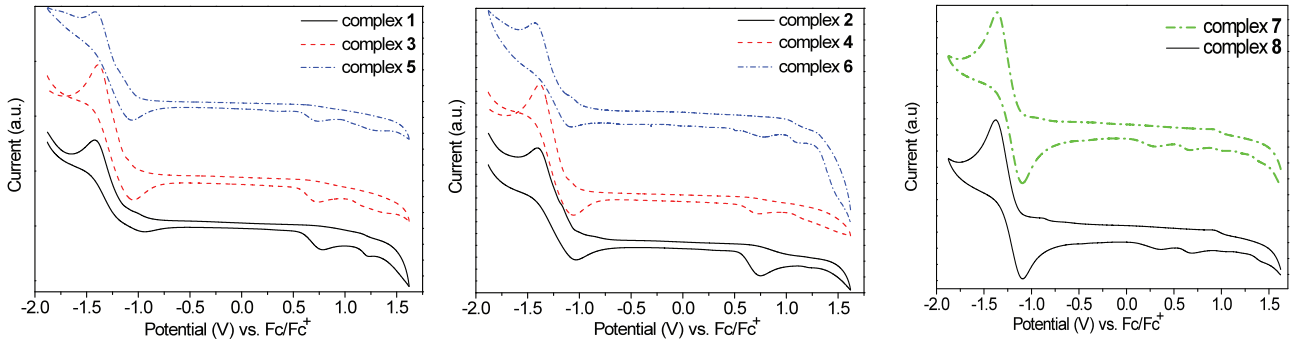

Figure 3. Cyclic voltammograms of complexes **1-8** in CH_3CN solutions (10^{-3} M). Potentials were recorded versus Fc/Fc^+.

Table 2. Electrochemical potentials and electronic energy levels.

Complex	E_{ox} [V][a)]	E_{red} [V][a)]	HOMO [eV][b)]	LUMO [eV][b)]	E_g^{CV} [eV][c)]
1	0.76	–1.42	–5.50	–3.32	2.18
2	0.75	–1.40	–5.49	–3.34	2.15
3	0.74	–1.38	–5.48	–3.36	2.12
4	0.74	–1.39	–5.48	–3.35	2.13
5	0.75	–1.42	–5.49	–3.32	2.17
6	0.77	–1.43	–5.51	–3.31	2.20
7	0.69	–1.38	–5.43	–3.36	2.07
8	0.67	–1.36	–5.41	–3.38	2.03

[a)]A glassy carbon electrode as the working electrode, an aqueous saturated calomel electrode as the operating reference electrode and a platinum wire as the counter electrode. Potentials are quoted versus ferrocene, 0.1 M Bu_4NPF_6 in CH_3CN solutions, scan rate = 100 mV s^{-1}; [b)]HOMO = $-e(E_{ox}+4.74)$[eV]; LUMO = $-e(E_{red}+4.74)$[eV]; [c)]$E_g^{CV} = e(E_{ox}-E_{red})$[eV].[51]

to **7** by replacing OXD with ppy. The oxidation potential can be independently adjusted by modification of the cyclometalated ligand. Complexes **7** and **8** exhibit oxidation peaks at +0.69 V and +0.67 V, respectively, which are lower than those of complexes **1-6** (+0.74 to +0.77 V). The electrochemical gaps, calculated from the difference between the anodic and cathodic peak potentials, for complexes **7** and **8** are smaller than those of complexes **1-6** (from 2.03 V for **8** to 2.20 V for **6**), which is consistent with the significantly red–shifted photoluminescence (PL) and electroluminescence (EL) from complexes **7** and **8**, compared to **1-6**.

2.4. Quantum Chemical Calculations

2.4.1. Calculation of the Ground States

Quantum chemical calculations were performed to gain insight into the photophysical and electrochemical behaviour of these cationic iridium complexes. The calculations on the ground and excited electronic states of the iridium complexes **1**, **2** and **7** were performed using density functional theory (DFT) and TDDFT at the B3LYP level. As shown in **Figure 4**, the HOMO of **1**, **2** and **7** resides on both the phenyl groups of the cyclometalated ligands and the iridium ions, while their LUMO resides on the ancillary ligands. For complexes **1** and **2**, their HOMO-1 and HOMO-2, with the metal contribution significantly reduced with respect to their HOMO, reside on the cyclometalated ligands and the iridium ions; their LUMO+1 and the LUMO+2 of complex **1** reside on the ancillary ligands and cyclometalated ligands; however, the LUMO+2 of complex **2** resides on the cyclometalated ligands.

Complexes **1** and **2** have the same subunits on which their HOMOs are localized (Ir and cyclometalated OXD ligands; Figure 4a,b) so, as expected, they show nearly the same oxidation potentials measured by cyclic voltammetry (Table 2). However, because of the electron-donating effect of $–CH_3$ substituents attached to the phenyl rings of the ancillary ligand, the LUMO energy level of complex **2** is increased, and therefore the energy gap is increased, and blue-shifted emission spectra are observed (16 nm in solution; 23 nm in film) relative to complex **1** (Table 1). Complex **7** has different cyclometalated ligands (ppy) than for complexes **1-6** (OXD), on which the HOMOs are localized. The calculated HOMO and LUMO energies of **7** are –7.96 eV and –5.06 eV, while those of **1** are –8.14 eV and –4.81 eV, respectively. As a result of the more electron-withdrawing and π-conjugated OXD ligand in complexes **1** and **2**, their HOMOs are significantly stabilized and the LUMOs are destabilized (**Figure 5**). The OXD group in the cyclometalated ligand of **1-6** plays a significant role in modifying the HOMO and LUMO levels. In the present study limited color tuning has been achieved with the structural modifications undertaken (Table 1).

The calculated energy gaps (LUMO–HOMO) of **1**, **2** and **7** are 3.29 eV, 3.33 eV, and 2.90 eV, respectively. The cyclometalated OXD ligands in **1** and **2** are more electron-withdrawing than the ppy ligands in **7**, with lower energy HOMOs but the LUMOs are destabilized. This is responsible for the wider HOMO-LUMO energy gap of **1** and **2** compared to **7**. The calculated results are in broad agreement with the trend in the experimental electrochemical data for the complexes, which shows a significantly larger E_g^{CV} values for **1** and **2** compared to **7** (Table 2). This is also consistent with the observed red shifted emission for **7** (Table 1).

2.4.2. Calculation of the Triplet-Excited States

To further investigate the nature of the emissive state of complexes **1** and **7** their low-lying triplet states were calculated at the optimized geometry of T_1 using the TDDFT approach. **Table 3** summarizes the vertical excitation energies and molecular orbitals involved in the dominant excitations. Additionally, the corresponding spin density distributions are displayed in Supporting Information Figure S4. TDDFT calculations show

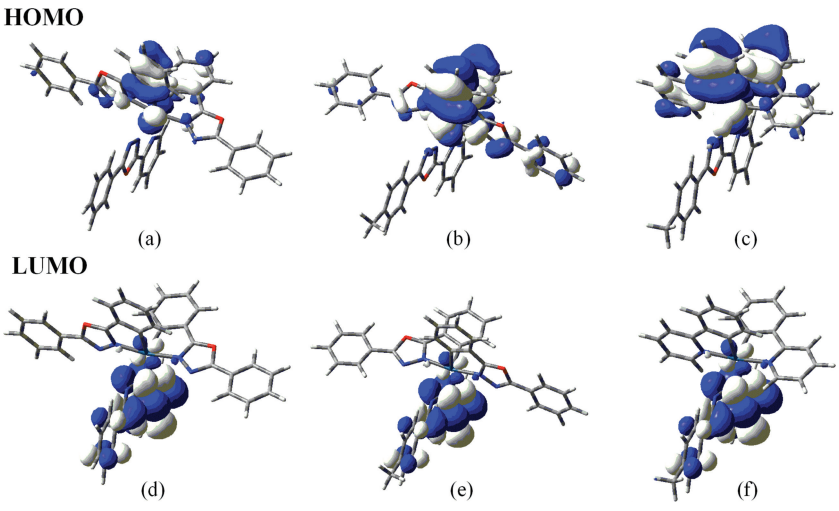

Figure 4. Optimized geometries and calculated molecular surfaces of complexes **1**, **2** and **7**. a–c): HOMOs of complexes **1**, **2** and **7**; d–f): LUMOs of complexes **1**, **2** and **7**.

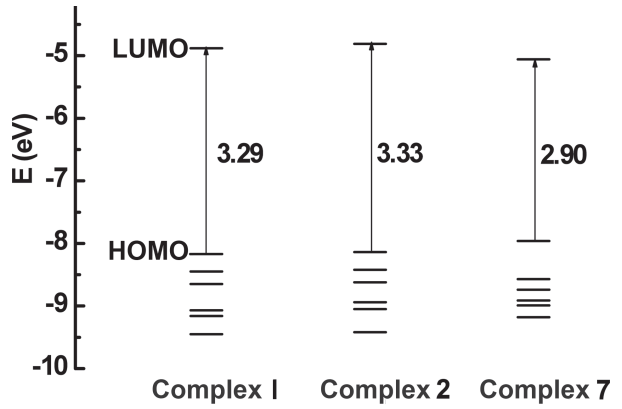

Figure 5. Calculated electronic structure for complexes **1**, **2** and **7** at their S_0 optimized geometries.

that the T_1 state for complexes **1** and **7** has characteristic mixed ^{3}MLCT (Ir → the ancillary ligands) and ^{3}LLCT (the cyclometalated ligands → the ancillary ligands) structure, which is also displayed by the spin density distributions (see Supporting Information Figure S4). For **7**, T_1 states involve predominantly the HOMO and LUMO orbitals while for **1** the HOMO-3 also takes part in the T_1 transition. Our calculated results are fully consistent with the experimental photoluminescence data, demonstrating that the emission is predominantly from ^{3}MLCT or ^{3}LLCT states.

Table 3. Selected triplet states for complexes **1** and **7** calculated from TDDFT approach.

Complex	States	E [eV][a]	Dominant Excitations[b]	Nature[c]
1	T_1	1.68	H→L(0.33)	$d_{Ir}+\pi_{OXD}\rightarrow\pi^*_{pop}$
			H-3→L(0.46)	$d_{Ir}+\pi_{pop}\rightarrow\pi^*_{pop}$
	T_2	2.10	H→L(0.60)	$d_{Ir}+\pi_{OXD}\rightarrow\pi^*_{pop}$
			H-1→L(0.13)	$d_{Ir}+\pi_{OXD}\rightarrow\pi^*_{pop}$
			H-3→L(0.12)	$d_{Ir}+\pi_{pop}\rightarrow\pi^*_{pop}$
	T_3	2.39	H-1→L(0.72)	$d_{Ir}+\pi_{OXD}\rightarrow\pi^*_{pop}$
			H-2→L(0.10)	$d_{Ir}+\pi_{OXD}\rightarrow\pi^*_{pop}$
	T_4	2.60	H-2→L(0.62)	$d_{Ir}+\pi_{OXD}\rightarrow\pi^*_{pop}$
			H-3→L(0.19)	$d_{Ir}+\pi_{pop}\rightarrow\pi^*_{pop}$
7	T_1	1.46	H→L(0.97)	$d_{Ir}+\pi_{ppy}\rightarrow\pi^*_{ptop}$
	T_2	2.00	H-4→L(0.73)	$d_{Ir}+\pi_{ptop}\rightarrow\pi^*_{ptop}$
	T_3	2.39	H-1→L(0.48)	$\pi_{ppy}\rightarrow\pi^*_{ptop}$
			H-3→L(0.12)	$d_{Ir}+\pi_{ptop}\rightarrow\pi^*_{ptop}$
			H-5→L(0.31)	$d_{Ir}+\pi_{ptop}\rightarrow\pi^*_{ptop}$
	T_4	2.54	H-1→L(0.45)	$\pi_{ppy}\rightarrow\pi^*_{ptop}$
			H-3→L(0.24)	$d_{Ir}+\pi_{ptop}\rightarrow\pi^*_{ptop}$
			H-5→L(0.26)	$d_{Ir}+\pi_{ptop}\rightarrow\pi^*_{ptop}$

[a]Excitation energies calculated for the triplet states; [b]H and L denote HOMO and LUMO, respectively; data in parentheses are the contributions of the corresponding excitations and only those higher than 0.10 are listed here; [c]Ligand notation: pop = 2-(5-phenyl-1,3,4-oxadiazol-2-yl)pyridine; ppy = 2-phenylpyridine; ptop = 2-(5-*p*-tolyl-1,3,4-oxadiazol-2-yl)pyridine.

For complex **7** the excitation energies of T_1–T_4 (1.46 eV, 2.00 eV, 2.39 eV, 2.54 eV) are lower than those of complex **1** (1.68 eV, 2.10 eV, 2.39 eV, 2.60 eV), clearly inferring that triplets are strongly confined on complex **7**.[53] The trend is consistent with the self-consistent-field (SCF) results as the values of T_1 by the SCF approach for **1** and **7** are 1.94 eV and 1.76 eV, respectively. A significant photoluminescence quantum yield (20%) is observed in films of complex **7**, while the value for **1** is only 10% (Table 1). Calculations therefore suggest that the device performance of **7** should be better than that of **1**, which is observed (**Table 4**).

2.5. Light-Emitting Cells (LECs)

To investigate the electroluminescent properties of these complexes, LECs based on complexes **1-8** were fabricated with a structure of ITO/PEDOT:PSS (50 nm)/cationic iridium complex: IL (molar ratio 4:1 w/w) (75 nm)/Al (120 nm). [PEDOT:PSS is (poly(3,4-ethylenedioxythiophene): poly(styrene sulfonate)]; IL is the ionic liquid 1-butyl-3-methylimidazolium hexafluorophosphate ($BMIMPF_6$)]. The PEDOT:PSS layer served to smooth the ITO surface and facilitate the hole injection, and the ionic liquid (IL) was added to enhance the ionic conductivity of the thin film and to reduce the turn-on time (t_{on}),[19] i.e., the time required to reach a luminance of 1 cd m^{-2}. With this structure, good reproducibility in electroluminescent performance was obtained for several on-off cycles. Details of the device preparation can be found in Section 4.2.

Figure 6 shows electroluminescent (EL) spectra of the LECs of **1-8**. For **1-6** EL peak values are in the range λ_{max} 552-564 nm; for **7** and **8** λ_{max} 616-624 nm (Table 4). The EL spectral profiles are similar to the PL spectra in thin films (Figure 2). For all the complexes **1-8** both the current density and brightness of the LECs increase gradually with time, which is a typical characteristic of LECs.[4] **Figure 7** shows representative data for the LECs of complexes **1** and **2**. The time required to reach the maximum brightness t_{max} depends on the complex layer thickness and the bias voltage. For complexes **1** and **2** with complex layer thickness of 75 nm t_{max} is 36 and 45 min at bias voltage of 6.5 and 5.7 V, respectively (Figure 7).

The characteristics of the LECs are summarized in Table 4. Device **4** exhibits the highest current efficiency (0.18 cd A^{-1}) of the yellow devices **1-6**; its maximum brightness is 22.0 cd m^{-2} under a bias voltage of 5.7 V, and the t_{max} is reached after only 5 min. However, its lifetime is very short: $t_{1/2}$ is only 12 min. In contrast, at this voltage the lifetime of device **2** ($t_{1/2}$ 260 min) which has the same ancillary ligand as device **4**, is the highest in the series **1-6**, but the t_{max} of **2** (45 min) is longer, and the maximum current efficiency (0.04 cd A^{-1}) is lower than for **4**. The LEC of complex **1** is the most efficient of the yellow complexes **1-6** reaching a maximum luminance of 3125 cd m^{-2} at a driving voltage of 14 V (Supporting Information Figure S5). A clear trend is that the red-emitting complexes **7** and **8** possess shorter turn-on times (1.5–2.5 min) compared to **1-6**, and the brightnesses of **7** and **8** (**7**: 217 cd m^{-2} and **8**: 154 cd m^{-2}) are considerably higher than for **1-6** under comparable conditions. Very high brightness of 8528 cd m^{-2} was obtained for complex **7** at device thickness 75 nm and biasing voltage of

Table 4. Electrical characteristics of LECs.[a)]

Complex	Conc. of complex [mg mL^{-1}]	Bias Voltage [V]	t_{max}[b)] [min]	$t_{1/2}$[c)] [min]	Lum$_{max}$ [cd m^{-2}]	EQE [%]	$\eta_{c,max}$ [cd A^{-1}]	EL λ_{max} [nm]	CIE[d)] (x,y)
1	15	6.5	36	83	12.0	0.03	0.082	560	(0.44,0.54)
2	16	5.7	45	260	10.1	0.01	0.045	552	(0.41,0.56)
3	15	5.7	27	133	22.2	0.03	0.087	556	(0.43,0.54)
4	16	5.7	5	12	22.0	0.06	0.18	552	(0.43,0.55)
5	20	5.7	5	20	19.4	0.005	0.018	564	(0.44,0.52)
6	20	5.7	5	17	12.9	0.006	0.021	560	(0.45,0.53)
7	20	5.0	72	590	217	2.74	6.29	616	(0.50,0.41)
8	20	5.0	35	490	154	9.51	13.05	624	(0.59,0.40)

[a)]The device structure is ITO/PEDOT: PSS (50 nm)/complex: $BMIMPF_6$ (molar ratio 4:1) (75 nm)/Al (120 nm); [b)]The time required to reach the maximum luminance; [c)]The time for the brightness of the device to decay from the maximum to half the maximum under a constant bias voltage; [d)]The CIE values were calculated with the software of a PR705 spectrophotometer.

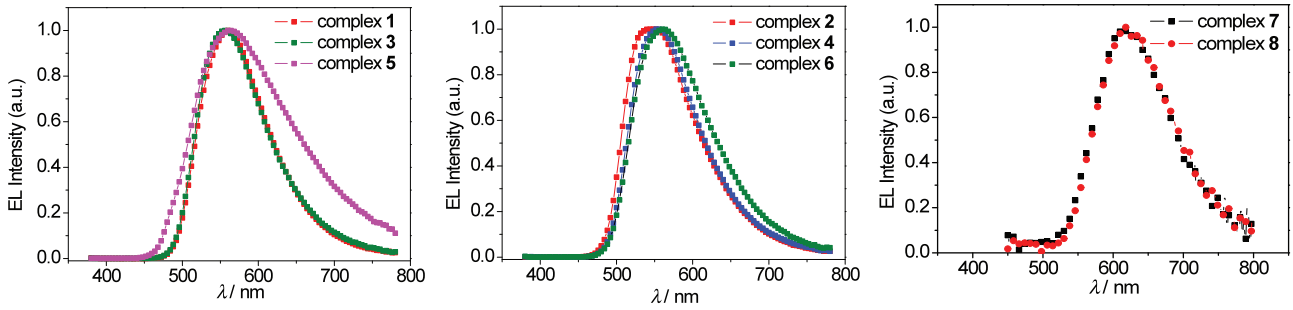

Figure 6. Electroluminescence spectra of LECs of complexes **1-8**. For the device structure see Table 4 footnote (a).

10 V (Supporting Information Figure S6). Another clear trend is that the beneficial effect of added ionic liquid is observed from the increased luminance for complex **7**, shown in Supporting Information Figure S6.

Complexes **7** and **8** display very high efficiencies for devices with a thicker emissive layer (210 nm; Supporting Information Figure S7). These two complexes are very similar with **7** being the slightly more efficient. Comprehensive characteristics of complex **7** were obtained at three different biasing voltages (3.5 V, 6 V and 10 V) as a function of time (Supporting Information Figure S7). The brightness, efficiencies and lifetimes ($t_{1/2}$) are all voltage dependent. The device external quantum efficiency (EQE) and device current efficiency (DevE) at low biasing voltage (3.5 V) were >10% and 3 cd A^{-1} at a brightness of 1 cd m^{-2}. These high values are mainly due to a low dark current <0.1 mA cm^{-2} (i.e., current that flows through the device without forming excitons) where most of the injected carriers recombine to give light, and also due to a low accumulation of

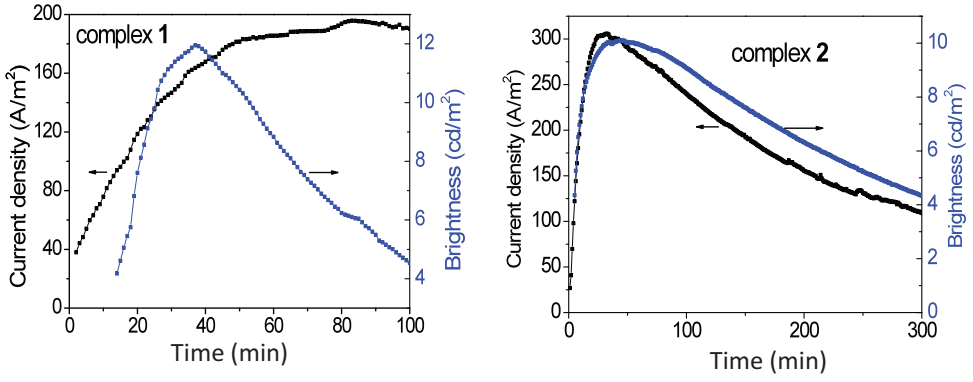

Figure 7. Time-dependent current density and brightness data for the LECs of complex **1** and complex **2** biased at 6.5 V and 5.7 V, respectively. For the device structure see Table 4 footnote (a).

ions near the electrodes at the early stage of the biasing. The maximum brightness at this low biasing voltage was obtained after 10 h (10 cd m^{-2}) and drops very slowly with time. As the biasing voltage increased to 6 V and 10 V the current density and the corresponding brightness also increases but the device $t_{1/2}$ decreases. This indicates that as the dark current increases at high voltage the device efficiencies are reduced.

To place these data in context, state of the art efficiencies for LECs have been reviewed recently.[2a] However, the efficiency of the red LECs of complexes **7** and **8** is impressive: the highest EQE quoted in the literature is 7.4%[2a] whereas complex **8** reaches 9.51% (Table 4).

3. Conclusions

In conclusion, eight new cationic iridium(III) complexes **1-8** all containing 2,5-diaryl-1,3,4-oxadiazole ligands have been prepared and their structural, photophysical, electrochemical and electroluminescent (EL) properties in LECs have been investigated. Systematically changing the substituents on the OXD ligands, or replacing the cyclometalated OXD ligand (**1-6**) with ppy (**7** and **8**), changes the PL and the EL properties of the devices. Complexes **1-6** are yellow emitters ($\lambda_{max,}$PL film 546-569 nm; EL 552-564 nm) whereas complexes **7** and **8** are red emitters ($\lambda_{max,}$ PL film 625-627 nm; EL 616-626 nm). A yellow LEC with maximum brightness of 3125 cd m^{-2} at 14 V has been achieved using **1** as the emitter. For red emission, LECs using **7** display very high efficiency or very high brightness depending on the active layer thickness and the bias voltage (EQE >10%, 210 nm active layer at 3.5 V, or 8528 cd m^{-2}, 75 nm active layer at 10 V). The efficiencies of **1-6** are low compared to the best performing yellow LECs.[2a] However, the efficiency data for **8** (peak EQE 9.51%) are comparable with the data reported by Tamayo et al for a red LEC (peak EQE 7.4%)[13a] which has been quoted in a recent review as the current state-of-the-art efficiency for red LECs.[2a] It should, however, be noted that in Tamayo's work[13a] very high brightness (7500 cd m^{-2}) was obtained at 3 V, while LECs of **7** attain this value–and even higher brightness–at higher voltages. The higher efficiencies for LECs of complexes **7** and **8** compared to **1-6** are ascribed to the single OXD ancillary ligand in **7** and **8** inducing less quenching of the MLCT transitions compared to the three OXD ligands in **1-6**. Also films of **7** and **8** have shorter excited state lifetimes compared to **1-6** and hence suffer less from excited state charge quenching during device operation. This work has, therefore, established that oxadiazole ligands are very promising components of iTMCs. Future work will involve optimization of ligand design to tune the emission color and to enhance the stability and efficiency of LECs for applications in EL device technology.

4. Experimental Section

General Information and Physical Measurements: All reactants and solvents were purchased from commercial sources. All chemicals were analytical grade and used without further purification. ^{1}H NMR spectra were recorded on a Bruker Avance 500 MHz spectrometer with tetramethylsilane as the internal standard at room temperature. Mass spectra were obtained using a Bruker Autoflex Speed MALDI-TOF spectrometer. Cyclic voltammetry was performed on a BAS 100 W instrument with a scan rate of 100 mV s^{-1} in CH_3CN (10^{-3} M) with the three-electrode configuration: a glassy carbon electrode as the working electrode, an aqueous saturated calomel electrode as the operating reference electrode and a platinum wire as the counter electrode. A solution of tetra-*n*-butylammonium tetrafluoroborate (0.1 M) in CH_3CN was used as the supporting electrolyte with ferrocene as the internal standard at room temperature. Photophysical data for complexes **1-8** in solution were obtained at room temperature using 5×10^{-5} M CH_2Cl_2 solutions; UV-vis absorption spectra were recorded on either a U3010 spectrometer (Hitachi, Japan) or a Shimadzu UV-3600 (UV-VIS-NIR) spectrophotometer; PL spectra were recorded on either a Cary Eclipse spectrofluorometer (Varian) equipped with a xenon lamp and quartz carrier or a Jobin-Yvon FLUOROMAX spectrofluorometer. Film quantum yields were measured using an integrating sphere (labsphere) following the described method.[50] Phosphorescence emission spectra and decays were collected using a N_2 laser (MNL 100, LTB) operating at 1–10 Hz. The excitation wavelength was 337.1 nm and the energy per pulse was kept below 100 μJ to avoid saturation effects. All measurements were performed under a dynamic vacuum of $<10^{-4}$ mbar in cryostat at room temperature. The light emitted by the sample was dispersed by a monochromator (TRIAX 190, Jobin Yvon-Spex) and recorded by a red enhanced, gated, intensified CCD camera (4 Picos, Stanford Computer Optics).

Device Preparation and Characterization: PEDOT:PSS is poly(3,4-ethylenedioxythiophene):poly(styrenesulfonate) (CLEVIOS P VP Al 4083 aqueous dispersion, 1.3–1.7% solid content Heraeus); solvents were obtained from Aldrich. Indium tin oxide (ITO)-coated glass substrates (20 Ω/□^{2}) were cleaned and treated with oxygen plasma before use. The PEDOT:PSS layer was spin-coated onto the ITO substrate and baked at 100 °C for 30 min, yielding a film with a thickness of ca. 50 nm. After cooling to room temperature, the solutions of complexes **1-6** and the ionic liquid ($BMIMPF_6$) in CH_2Cl_2 were spin coated onto the substrate, and then the light emitting layer with a thickness of ca 75 nm was baked at 80 °C for 2 h. For complexes **7** and **8** a solution of mixed solvent 1:1 v/v acetonitrile:benzene was used. The film was transferred into a metal evaporating chamber where an aluminum cathode (120 nm) was evaporated under low pressure ($<5 \times 10^{-4}$ mbar). The EL spectra were obtained with a Photo Research PR650 spectrophotometer in ambient conditions. The lifetime data were obtained by applying a constant voltage using a Keithley 2400 source meter and measuring the current density and brightness as a function of time. Devices employing complexes **7** and **8** prepared and characterized in the Physics Department, Durham University, were encapsulated inside the glove box using DELO UV cured epoxy (KATIOBOND) and capped with 1.2 × 1.2 cm microscope glass slide then exposed to UV light for 3 min. The current-voltage (*I-V*) characteristics and the emission intensities were measured in a calibrated integrating sphere and the data acquisition was controlled using a home-written NI LabView program which controlled an Agilent Technologies 6632B power supply. The electroluminescence (EL) spectra were measured using an Ocean Optics USB 4000 CCD spectrometer supplied with 400 μm UV/vis fiber optic cable.

Synthesis and Characterization of the Ir Complexes: The synthesis of the ligands is described in the Supporting Information. The dimeric iridium(III) intermediates of general formula $(C^\wedge N)_2Ir(\mu\text{-}Cl)_2Ir(C^\wedge N)_2$ were synthesized by the standard procedure.[47]

$[Ir(OXD)_2(pop)]^+(PF_6^-)$ (complex **1***)*: 2,5-Diphenyl-1,3,4-oxadiazole (0.666 g, 3.0 mmol) and $IrCl_3{\cdot}3H_2O$ (0.352 g, 1.0 mmol) were dissolved in 2-ethoxyethanol (30 mL) and distilled water (10 mL). The mixture was refluxed at 120 °C for 24 h under a nitrogen atmosphere and then cooled to room temperature. The dichloro-bridged diiridium complex $[Ir(OXD)_2Cl]_2$ was obtained by filtration and was washed sequentially with distilled water, ethanol and ether. A suspension of $[Ir(OXD)_2Cl]_2$ (0.202 g, 0.15 mmol) and 2-(5-phenyl-1,3,4-oxadiazol-2-yl)pyridine (pop) (0.067 g, 0.30 mmol) in EtOH (15 mL) and CH_2Cl_2 (15 mL) was refluxed under an inert nitrogen atmosphere in the dark at 78 °C for 4 h. After cooling to room temperature, solid potassium hexafluorophosphate

(0.083 g, 0.45 mmol) was added to the solution. The mixture was stirred for 30 min at room temperature. The suspension was then filtered and the precipitate was washed with petroleum ether and dried. The crude product was recrystallized from petroleum ether to yield complex **1** as a yellow solid (0.054 g, 71% yield). ^{1}H NMR (500 MHz, $CDCl_3$, δ [ppm]): 8.72 (d, *J* = 8.5 Hz, 1H), 8.43 (t, *J* = 7.0 Hz, 1H), 8.23 (d, *J* = 8.0 Hz, 2H), 8.09 (d, *J* = 7.5 Hz, 2H), 8.04 (d, *J* = 7.5 Hz, 2 H), 7.69-7.76 (m, 2H), 7.59-7.63 (m, 2H), 7.26-7.57 (m, 8H), 7.10-7.20 (m, 5H), 6.78-6.82 (m, 2H). MS (MALDI-TOF) [m/z]: 858.2 $(M\text{-}PF_6)^+$. Anal. Calcd. for $C_{41}H_{27}F_6IrN_7O_3P$: C 49.10, H 2.71, N 9.78. Found C 49.06, H 2.77, N 9.72. Crystals for X-ray analysis were obtained by slow evaporation of a dichloromethane-methanol solution of **1**.

[Ir(OXD)$_2$(ptop)]$^+$(PF$_6^-$) (complex **2***)*: The synthesis of complex **2** was similar to that of complex **1** except that the ancillary ligand pop was replaced by 2-(5-*p*-tolyl-1,3,4-oxadiazol-2-yl)pyridine (ptop). Complex **2** was obtained as a yellow solid (0.057 g, 75% yield). ^{1}H NMR (500 MHz, $CDCl_3$, δ [ppm]): 8.68 (d, *J* = 8.0 Hz, 1H), 8.43 (t, *J* = 7.0 Hz, 1H), 8.09 (t, *J* = 5.0 Hz, 4H), 8.04 (d, *J* = 7.5 Hz, 2H), 7.67-7.76 (m, 3H), 7.50-7.60 (m, 6H), 7.35 (d, *J* = 8.0 Hz, 2H), 7.10-7.21 (m, 5H), 6.78-6.82 (m, 2H), 2.44 (s, 3H). MS (MALDI-TOF) [m/z]: 872.2 $(M\text{-}PF_6)^+$. Anal. Calcd. for $C_{42}H_{29}F_6IrN_7O_3P$: C 49.61, H 2.87, N 9.64. Found C 49.64, H 2.82, N 9.60. Crystals for X-ray analysis were obtained by slow evaporation of a dichloromethane-methanol solution of **2**.

[Ir(dcOXD)$_2$(pop)]$^+$(PF$_6^-$) (complex **3***)*: The synthesis of complex **3** was similar to that of complex **1** except that $[Ir(OXD)_2Cl]_2$ was replaced by the dimethyl analogue $[Ir(dcOXD)_2Cl]_2$. Complex **3** was obtained as a yellow solid (0.061 g, 77% yield). ^{1}H NMR (500 MHz, $CDCl_3$, δ [ppm]): 8.70 (d, *J* = 8.0 Hz, 1H), 8.42 (t, *J* = 7.5 Hz, 1H), 8.23 (d, *J* = 5 Hz, 2H), 8.06 (d, *J* = 5.5 Hz, 1H), 7.96 (d, *J* = 8.0 Hz, 2H), 7.91 (d, *J* = 8.5 Hz, 2H), 7.69 (t, *J* = 7.5 Hz, 1H), 7.62 (t, *J* = 8.0 Hz, 3H), 7.55 (t, *J* = 7.5 Hz, 2H), 7.31 (t, *J* = 7.5 Hz, 4H), 7.00 (d, *J* = 7.0 Hz, 1H), 6.96 (d, *J* = 8.0 Hz, 1H), 6.57 (d, *J* = 14.5 Hz, 2H), 2.43 (s, 6H), 2.31 (s, 3H), 2.29 (s, 3H). MS (MALDI-TOF) [m/z]: 914.2 $(M\text{-}PF_6)^+$. Anal. Calcd. for $C_{45}H_{35}F_6IrN_7O_3P$: C 51.04, H 3.33, N 9.26. Found C 51.06, H 3.24, N 9.19.

[Ir(dcOXD)$_2$(ptop)]$^+$(PF$_6^-$) (complex **4***)*: The synthesis of complex **4** was similar to that of complex **3** except that the ancillary ligand pop was replaced with ptop. Complex **4** was obtained as a yellow solid (0.058 g, 72% yield). ^{1}H NMR (500 MHz, $CDCl_3$, δ [ppm]): 8.66 (d, *J* = 8.0 Hz, 1H), 8.42 (t, *J* = 7.5 Hz, 1H), 8.10 (d, *J* = 8.5 Hz, 2H), 8.05 (d, *J* = 4 Hz, 1H), 7.96 (d, *J* = 8.5 Hz, 2H), 7.91 (d, *J* = 8.0 Hz, 2H), 7.68 (t, *J* = 7.0 Hz, 1H), 7.63 (t, *J* = 8.0 Hz, 2H), 7.26-7.35 (m, 6H), 7.00 (d, *J* = 8.0 Hz, 1H), 6.95 (d, *J* = 7.5 Hz, 1H), 6.57 (d, *J* = 18 Hz, 2H), 2.43 (s, 3H), 2.42 (s, 3H), 2.42 (s, 3H), 2.31 (s, 3H), 2.28 (s, 3H). MS (MALDI-TOF) [m/z]: 928.3 $(M\text{-}PF_6)^+$. Anal. Calcd. for $C_{46}H_{37}F_6IrN_7O_3P$: C 51.49, H 3.48, N 9.14. Found C 51.53, H 3.39, N 9.20.

[Ir(dmOXD)$_2$(pop)]$^+$(PF$_6^-$) (complex **5***)*: The synthesis of complexes **5** was similar to that of complex **1** except that $[Ir(OXD)_2Cl]_2$ was replaced by the dimethoxy analogue $[Ir(dmOXD)_2Cl]_2$. Complex **5** was obtained as a yellow solid (0.063 g, 74% yield). ^{1}H NMR (500 MHz, $CDCl_3$, δ [ppm]): 8.67 (d, *J* = 8.0 Hz, 1H), 8.41 (t, *J* = 7.0 Hz, 1H), 8.23 (d, *J* = 7.0 Hz, 2H), 8.14 (d, *J* = 5.5 Hz, 1H), 7.97 (d, *J* = 9.0 Hz, 2 H), 7.92 (d, *J* = 8.5 Hz, 2H), 7.57-7.69 (m, 4H), 7.56 (t, 7.5 Hz, 2H), 6.98 (m, 4H), 6.68-6.75 (m, 2H), 6.28 (m, 2H), 3.87 (s, 3H), 3.86 (s, 3H), 3.75 (s, 3H), 3.73 (s, 3H). MS (MALDI-TOF) [m/z]: 978.2 $(M\text{-}PF_6)^+$. Anal. Calcd. for $C_{45}H_{35}F_6IrN_7O_7P$: C 48.13, H 3.14, N 8.73. Found C 48.09, H 3.21, N 8.67.

[Ir(dmOXD)$_2$(ptop)]$^+$(PF$_6^-$) (complex **6***)*: The synthesis of complex **6** was similar to that of complex **5** except that the ancillary ligand pop was replaced with ptop. Complex **6** was obtained as a yellow solid (0.067 g, 78% yield). ^{1}H NMR (500 MHz, $CDCl_3$, δ [ppm]): 8.63 (d, *J* = 7.5 Hz, 1H), 8.40 (t, *J* = 7.0 Hz, 1H), 8.13 (d, *J* = 5.0 Hz, 1H), 8.10 (d, *J* = 8.0 Hz, 2H), 7.96 (d, *J* = 9.0 Hz, 2 H), 7.93 (d, *J* = 8.5 Hz, 2H), 7.65-7.70 (m, 3H), 7.35 (d, 7.5 Hz, 2H), 6.98 (t, *J* = 8.0 Hz, 4H), 6.68-6.74 (m, 2H), 6.29 (d, *J* = 2.5 Hz, 1H), 6.27 (d, *J* = 2.0 Hz, 1H), 3.87 (s, 3H), 3.86 (s, 3H), 3.75 (s, 3H), 3.73 (s, 3H), 2.44 (s, 3H). MS (MALDI-TOF) [m/z]: 992.2 $(M\text{-}PF_6)^+$. Anal. Calcd. for $C_{46}H_{37}F_6IrN_7O_7P$: C 48.59, H 3.28, N 8.62. Found C 48.43, H 3.33, N 8.70..

[Ir(ppy)$_2$(ptop)]$^+$(PF$_6^-$) (complex **7***)*: A mixture of dichloro-bridged diiridium complex $[Ir(ppy)_2Cl]_2$[49a] (0.2152 g, 0.20 mmol) and 2-(5-*p*-tolyl-[1,3,4]oxadiazol-2-yl)-pyridine (ptop) (0.095 g, 0.4 mmol) in methanol/ dichloromethane (40 mL) (1:1 v/v) was refluxed under an inert atmosphere of nitrogen in the dark for 4 h. The yellow solution was then cooled to room temperature, and KPF_6 (75 mg, 0.4 mmol) was added. The mixture was stirred for 30 min at room temperature and then evaporated to dryness. The yellow solid was dissolved in dichloromethane and purified by column chromatography on alumina (CH_2Cl_2 + 1% MeOH as eluent) to yield complex **7** as a yellow powder (0.125 g, 68% yield). ^{1}H NMR (500 MHz, DMSO-d_6, δ [ppm]): 8.68 (d, *J* = 8.0 Hz, 1H), 8.38-8.41(m, 1H), 8.28 (d, *J* = 5.5 Hz, 1H), 8.24 (d, *J* = 8.0 Hz, 2H), 8.03 (d, *J* = 8.5 Hz, 2H), 7.96 (t, *J* = 7.5 Hz, 2H), 7.90 (d, *J* = 8.0 Hz, 1H), 7.83-7.86 (m, 3H), 7.65 (d, *J* = 5.5 Hz, 1H), 7.46 (d, *J* = 8.5 Hz, 2H), 7.19-7.22 (m, 2H), 7.03 (t, *J* = 8.0 Hz, 1H), 6.95-6.97 (m, 1H), 6.91 (t, *J* = 7.5 Hz, 1H), 6.81-6.84 (m, 1H), 6.11-6.14 (m, 1H), 2.42 (s, 3H). MS (MALDI-TOF) [m/z]: 738.2 $(M\text{-}PF_6)^+$. Anal. Calcd. for $C_{36}H_{27}F_6IrN_5OP$: C 48.98, H 3.08, N 7.93. Found C 48.54, H 3.12, N 7.89. Crystals for X-ray analysis were obtained by slow evaporation of a dichloromethane-methanol solution of **7**.

[Ir(ppy)$_2$(pop)]$^+$(PF$_6^-$) (complex **8***)*: Following the procedure for complex **7**, $[Ir(ppy)_2Cl]_2$ (0.2152 g, 0.2 mmol) and 2-(5-phenyl-[1,3,4] oxazdiazol-2-yl)-pyridine (pop) (0.095g, 0.4 mmol) in methanol/ dichloromethane (40 mL) (1:1 v/v), followed by KPF_6 (75 mg, 0.4 mmol) gave complex **8** as a yellow powder (0.120 g, 65%). ^{1}H NMR (500 MHz, DMSO-d_6, δ [ppm]): 8.70 (d, *J* = 7.5 Hz, 1H), 8.39-8.42(m, 1H), 8.28(d, *J* = 5.0 Hz, 1H), 8.24 (d, *J* = 8.5 Hz, 2H), 8.14 (d, *J* = 7.5 Hz, 2 H), 7.96 (t, *J* = 7.5 Hz, 2H), 7.90 (d, *J* = 7.0 Hz, 1H), 7.86 (t, *J* = 2.5 Hz, 3H), 7.74 (t, *J* = 8.0 Hz, 1H), 7.65 (t, *J* = 8.0 Hz, 3H), 7.18-7.22 (m, 2H), 7.03 (t, *J* = 7.0 Hz, 1H), 6.95-6.98 (m, 1H), 6.91 (t, *J* = 7.5 Hz, 1H), 6.83 (t, *J* = 7.5 Hz, 1H), 6.13(t, *J* = 7.5 Hz, 1H). MS (MALDI-TOF) [m/z]: 724.2 $(M\text{-}PF_6)^+$. Anal. Calcd. for $C_{35}H_{25}F_6IrN_5OP$: C 48.39, H 2.90, N 8.06. Found: C 48.42, H 2.88, N 8.12. Crystals for X-ray analysis were obtained by slow evaporation of a dichloromethane-methanol solution of **8**.

X-Ray Crystallography: Crystallographic data (excluding structure factors) have been deposited with the Cambridge Crystallographic Data Centre as supplementary publication numbers 886442 (complex **1**), 886443 (complex **2**), 890732 (complex **7**) and 890723 (complex **8**). Copies of the data can be obtained free of charge from www.ccdc.cam.ac.uk/conts/retrieving.html or on application to The Director, Cambridge Crystallographic Data Centre (CCDC), 12 Union Road, Cambridge CB2 1EZ, UK. E-mail: deposit@ccdc.cam.ac.uk; www.ccdc.cam.ac.uk.

Supporting Information

Supporting Information is available from the Wiley Online Library or from the author.

Acknowledgements

J.Z. and L.Z. contributed equally to the work reported in this article. The work in China was funded by NSFC (51203017, 21131001), the Science and Technology Development Planning of Jilin Province (20100540) and NENU-STC08012. The work in Durham was funded by EPSRC.

Received: January 28, 2013
Revised: February 25, 2013
Published online: April 18, 2013

[1] a) R. D. Costa, E. Ortí, D. Tordera, A. Pertegás, H. J. Bolink, S. Graber, C. E. Housecroft, L. Sachno, M. Neuburger, E. C. Constable, *Adv. Energy Mater.* **2011**, *1*, 282; b) W. J. Xu, S. J. Liu, T. C. Ma, Q. Zhao, A. Pertegás, D. Tordera, H. J. Bolink, S. H Ye, X. M Liu, S. Sun, W. Huang, *J. Mater. Chem.* **2011**, *21*, 13999.

[2] a) T. Hu, L. He, L. Duan, Y. Qiu, *J. Mater. Chem.* **2012**, *22*, 4206; b) D. Tordera, S. Meier, M. Lenes, R. D. Costa, E. Ortí, W. Sarfert, H. J. Bolink, *Adv. Mater.* **2012**, *24*, 897; c) S. B. Meier, W. Sarfert, J. M. Junquera-Hernández, M. Delgado, D. Tordera, E. Ortí, H. J. Bolink, F. Kessler, R. Scopelliti, M. Grätzel, M. K. Nazeeruddind, E. Baranoff, *J. Mater. Chem. C* **2013**, *1*, 58.

[3] a) X. Zeng, M. Tavasli, I. F. Perepichka, A. S. Batsanov, M. R. Bryce, C. Chiang, C. Rothe, A. P. Monkman, *Chem. Eur. J.* **2008**, *14*, 933; b) R. D. Costa, E. Ortí, H. J. Bolink, S. Graber, C. E. Housecroft, E. C. Constable, *Chem. Commun.* **2011**, *47*, 3207; c) T. Hu, L. Duan, J. Qiao, L. He, D. Q. Zhang, R. J. Wang, L. D. Wang, Y. Qiu, *Org. Electron.* **2012**, *13*, 1948; d) L. He, L. Duan, J. Qiao, D. Q. Zhang, L. D. Wang, Y. Qiu, *Chem. Commun.* **2011**, *47*, 6467.

[4] Q. B. Pei, G. Yu, C. Zhang, Y. Yang, A. J. Heeger, *Science* **1995**, *269*, 1086.

[5] J. K. Lee, D. S. Yoo, E. S. Handy, M. F. Rubner, *Appl. Phys. Lett.* **1996**, *69*, 1686.

[6] J. D. Slinker, J. A. Defranco, M. J. Jaquith, W. R. Silveira, Y. W. Zhong, J. M. Moran-Mirabal, H. G. Craighead, H. D. Abruña, J. A. Marohn, G. G. Malliaras, *Nat. Mater.* **2007**, *6*, 894.

[7] a) C. H. Lyons, E. D. Abbas, J. K. Lee, M. F. Rubner, *J. Am. Chem. Soc.* **1998**, *120*, 12100; b) E. S. Handy, A. J. Pal, M. F. Rubner, *J. Am. Chem. Soc.* **1999**, *121*, 3525; c) F. G. Gao, A. J. Bard, *J. Am. Chem. Soc.* **2000**, *122*, 7426; d) H. Rudmann, M. F. Rubner, *J. Appl. Phys.* **2001**, *90*, 4338; e) C. Y. Liu, A. J. Bard, *J. Am. Chem. Soc.* **2002**, *124*, 4190; f) H. Rudmann, S. Shimada, M. F. Rubner, *J. Am. Chem. Soc.* **2002**, *124*, 4918; g) M. Buda, G. Kalyuzhny, A. J. Bard, *J. Am. Chem. Soc.* **2002**, *124*, 6090; h) S. Bernhard, J. A. Barron, P. L. Houston, H. D. Abruña, J. L. Ruglovksy, X. C. Gao, G. G. Malliaras, *J. Am. Chem. Soc.* **2002**, *124*, 13624; i) G. Kalyuzhny, M. Buda, J. McNeill, P. Barbara, A. J. Bard, *J. Am. Chem. Soc.* **2003**, *125*, 6272; j) C. Y. Liu, A. J. Bard, *Appl. Phys. Lett.* **2005**, *87*, 061110; k) D. L. Pile, A. J. Bard, *Chem. Mater.* **2005**, *17*, 4212; l) W. Zhao, C. Y. Liu, Q. Wang, J. M. White, A. J. Bard, *Chem. Mater.* **2005**, *17*, 6403; m) H. J. Bolink, L. Cappelli, E. Coronado, P. Gaviña, *Inorg. Chem.* **2005**, *44*, 5966; n) H. J. Bolink, L. Cappelli, E. Coronado, M. Grätzel, M. K. Nazeeruddin, *J. Am. Chem. Soc.* **2006**, *128*, 46; o) L. J. Soltzberg, J. D. Slinker, S. Flores-Torres, D. A. Bernards, G. G. Malliaras, H. D. Abruña, J. Kim, R. H. Friend, M. D. Kaplan, V. Goldberg, *J. Am. Chem. Soc.* **2006**, *128*, 7761; p) J. D. Slinker, J. Rivnay, J. A. DeFranco, D. A. Bernards, A. A. Gorodetsky, S. T. Parker, M. P. Cox, R. Rohl, G. G. Malliaras, Flores-Torres, H. D. Abruña, *J. Appl. Phys.* **2006**, *99*, 074502; q) R. D. Costa, E. Ortí, H. J. Bolink, F. Monti, G. Accorsi, N. Armaroli, *Angew. Chem. Int. Ed.* **2012**, *51*, 8178.

[8] a) F. G. Gao, A. J. Bard, *Chem. Mater.* **2002**, *14*, 3465; b) S. Bernhard, X. C. Gao, G. G. Malliaras, H. D. Abruña, *Adv. Mater.* **2002**, *14*, 433; c) A. R. Hosseini, C. Y. Koh, J. D. Slinker, S. Flores-Torres, H. D. Abruña, G. G. Malliaras, *Chem. Mater.* **2005**, *17*, 6114.

[9] a) Y. M. Wang, F. Teng, Y. B. Hou, Z. Xu, Y. S. Wang, W. F. Fu, *Appl. Phys. Lett.* **2005**, *87*, 233512; b) N. Armaroli, G. Accorsi, M. Holler, O. Moudam, J. F. Nierengarten, Z. Y. Zhou, R. T. Wegh, R. Welter, *Adv. Mater.* **2006**, *18*, 1313; c) Q. S. Zhang, Q. G. Zhou, Y. X. Cheng, L. X. Wang, D. G. Ma, X. B. Jing, F. S.Wang, *Adv. Funct. Mater.* **2006**, *16*, 1203; d) R. D. Costa, D. Tordera, E. Ortí, H. J. Bolink, J. Schönle, S. Graber, C. E. Housecroft, E. C. Constable, J. A. Zampese, *J. Mater. Chem.* **2011**, *21*, 16108.

[10] J. D. Slinker, C. Y. Koh, G. G. Malliaras, M. S. Lowry, S. Bernhard, *Appl. Phys. Lett.* **2005**, *86*, 173506.

[11] a) C. T. Liao, H. F. Chen, H. C. Su, K. T. Wong, *J. Mater. Chem.* **2011**, *21*, 17855; b) H. F. Chen, W.Y. Hung, S.W. Chen, T. C. Wang, S. W. Lin, S. H. Chou, C. T. Liao, H. C. Su, H. A. Pan, P. T. Chou, Y. H. Liu, K. T. Wong, *Inorg. Chem.* **2012**, *51*, 12114; c) L. F. Sun, A. Galan, S. Ladouceur, J. D. Slinker, E. Zysman-Colman, *J. Mater. Chem.* **2011**, *21*, 18083; d) E. Baranoff, H. J. Bolink, E. C. Constable, M. Delgado, D. Häussinger, C. E. Housecroft, M. K. Nazeeruddin, M. Neuburger, E. Ortí, G. E. Schneider, D. Tordera, R. M. Walliser, J. A. Zampese, *Dalton Trans.* **2013**, *42*, 1073; e) H. C. Su, H. F. Chen, P. H. Chen, S.W. Lin, C. T. Liao, K. T. Wong, *J. Mater. Chem.* **2012**, *22*, 22998.

[12] a) M. S. Lowry, J. I. Goldsmith, J. D. Slinker, R. Rohl, R. A. Pascal Jr, G. G. Malliaras, S. Bernhard, *Chem. Mater.* **2005**, *17*, 5712; b) C.H. Yang, J. Beltran, V. Lemaur, J. Cornil, D. Hartmann, W. Sarfert, R. Fröhlich, C. Bizzarri, L. D. Cola, *Inorg. Chem.* **2010**, *49*, 9891; c) H. B. Wu, H.F. Chen, C.T. Liao, H.C. Su, K.T. Wong, *Org. Electron.* **2012**, *13*, 483.

[13] a) A. B. Tamayo, S. Garon, T. Sajoto, P. I. Djurovich, I. M. Tsyba, R. Bau, M. E. Thompson, *Inorg. Chem.* **2005**, *44*, 8723; b) F. Kessler, R. D. Costa, D. Di Censo, R. Scopelliti, E. Ortí. H. J. Bolink, S. Meier, W. Sarfert, M. Grätzel, Md. K. Nazeeruddin, E. Baranoff, *Dalton Trans.* **2012**, *41*, 180; c) H. B. Wu, H.F. Chen, C.T. Liao, H.C. Su, K.T. Wong, *Org. Electron.* **2012**, *13*, 483.

[14] Md. K. Nazeeruddin, R. T. Wegh, Z. Zhou, C. Klein, Q. Wang, F. De Angelis, S. Fantacci, M. Grätzel, *Inorg. Chem.* **2006**, *45*, 9245; b) M. S. Lowry, W. R. Hudson, R. A. Pascal Jr., S. Bernhard, *J. Am. Chem. Soc.* **2004**, *126*, 14129.

[15] F. De Angelis, S. Fantacci, N. Evans, C. Klein, S. M. Zakeeruddin, Jacques-E. Moser, K. Kalyanasundaram, H. J. Bolink, M. Grätzel, M. K. Nazeeruddin, *Inorg. Chem.* **2007**, *46*, 5989.

[16] H. J. Bolink, L. Cappelli, E. Coronado, A. Parham, P. Stössel, *Chem. Mater.* **2006**, *18*, 2778.

[17] a) H. J. Bolink, L. Cappelli, S. Cheylan, E. Coronado, R. D. Costa, N. Lardiés, Md. K. Nazeeruddin, E. Ortí, *J. Mater. Chem.* **2007**, *17*, 5032; b) J. D. Slinker, A. A. Gorodetsky, M. S. Lowry, J. J. Wang, S. Parker, R. Rohl, S. Bernhard, G. G. Malliaras, *J. Am. Chem. Soc.* **2004**, *126*, 2763.

[18] a) H. C. Su, F. C. Fang, T. Y. Hwu, H. H. Hsieh, H. F. Chen, G. H. Lee, S. M. Peng, K. T. Wong, C. C. Wu, *Adv. Funct. Mater.* **2007**, *17*, 1019; b) K. A. King, R. J. Watts, *J. Am. Chem. Soc.* **1987**, *109*, 1589.

[19] S. T. Parker, J. D. Slinker, M. S. Lowry, M. P. Cox, S. Bernhard, G. G. Malliaras, *Chem. Mater.* **2005**, *17*, 3187.

[20] a) D. Di Censo, S. Fantacci, F. De Angelis, C. Klein, N. Evans, K. Kalyanasundaram, H. J. Bolink, M. Grätzel, M. K. Nazeeruddin, *Inorg. Chem.* **2008**, *47*, 980; b) E. Margapoti, M. Muccini, A. Sharma, A. Colombo, C. Dragonetti, D. Robertob, A. Valore, *Dalton Trans.* **2012**, *41*, 9227; c) E. Margapoti, V. Shukla, A. Valore, A. Sharma, C. Dragonetti, C. C. Kitts, D. Roberto, M. Murgia, R. Ugo, M. Muccini*J. Phys. Chem. C* **2009**, *113*, 12517; d) R. D. Costa, E. Ortí, H. J. Bolink, S. Graber, C. E. Housecroft, M. Neuburger, S. Schaffner, E. C. Constable, *Chem. Commun.* **2009**, *15*, 2029.

[21] X. Zeng, M. Tavasli, A. S. Batsanov, I. F. Perepichka, M. R. Bryce, C. J. Chiang, C. Rothe, A. P. Monkman, *Chem. Eur. J.* **2008**, *14*, 933.

[22] H. C. Su, H. F. Chen, C. C. Wu, K. T. Wong, *Chem. Asian J.* **2008**, *3*, 1922.

[23] S. Graber, K. Doyle, M. Neuburger, C. E. Housecroft, E. C. Constable, R. D. Costa, E. Ortí, D. Repetto, H. J. Bolink, *J. Am. Chem. Soc.* **2008**, *130*, 14944.

[24] V. Marin, E. Holder, R. Hoogenboom, U. S. Schubert, *Chem. Soc. Rev.* **2007**, *36*, 618.

[25] T. Sajoto, P. I. Djurovich, A. Tamayo, M. Yousufuddin, R. Bau, M. E.Thompson, R. J. Holmes, S. R. Forrest, *Inorg. Chem.* **2005**, *44*, 7992.

[26] F. Neve, M. La Deda, A. Crispini, A. Bellusci, F. Puntoriero, S. Campagna, *Organometallics* **2004**, *23*, 5856.

[27] L. Wang, B. Du, Y. Cao, J. Wang, *Proc. SPIE* **2007**, *6828*, 68280I.

[28] H. Su, C. Wu, F. Fang, K. Wong, *Appl. Phys. Lett.* **2006**, *89*, 261118.

[29] H. Su, H. Chen, F. Fang, C. Liu, C. Wu, K. Wong, Y. Liu, S. Peng, *J. Am. Chem. Soc.* **2008**, *130*, 3413.

[30] L. He, L. Duan, J. Qiao, R. Wang, P. Wei, L. Wang, Y. Qiu, *Adv. Funct. Mater.* **2008**, *18*, 2123.

[31] a) C. Rothe, C. Chiang, V. Jankus, K. Abdullah, X. Zeng, R. Jitchati, A. S. Batsanov, M. R. Bryce, A. P. Monkman, *Adv. Funct. Mater.* **2009**, *19*, 2038; b) D. Tordera, A. Perteg, N. Shavaleev, R. Scopelliti, E. Ortí, H. J. Bolink, E. Baranoff, M. Grätzel, M. K. Nazeeruddin, *J. Mater. Chem.* **2012**, *22*, 19264.

[32] G. Volpi, C. Garino, E. Breuza, R. Gobetto, C. Nervi, *Dalton Trans.* **2012**, *41*, 1065.

[33] V. Chandrasekhar, T. Hajra, J. K. Bera, S. M. Wahidur Rahaman, N. Satumtira, O. Elbjeirami, M. A. Omary, *Inorg. Chem.* **2012**, *51*, 1319.

[34] a) E. Puodziukynaite, J. L. Oberst, A. L. Dyer, J. R. Reynolds, *J. Am. Chem. Soc.* **2012**, *134*, 968; b) G. Santos, F. Fonseca, A. M. Andrade, A. O. T. Patrocínio, S. K. Mizoguchi, N. Y. Murakami Iha, M. Peres, T. Monteiro, L. Pereira, *Phys. Status Solidi A* **2008**, *205*, 2057; c) H. J. Bolink, E. Coronado, R. D. Costa, P. Gaviña, E. Ortí, S. Tatay, *Inorg. Chem.* **2009**, *48*, 3907; d) G. Santos, F.J. Fonseca, A.M. Andrade, A. O. T. Patrocínio, S. K. Mizoguchi, N. Y. MurakamiIha, M. Peres, W. Simöes, Monteiro L. Pereira, *J. Non-Cryst. Solids* **2008**, *354*, 2571; e) C. C. Ju, C. H. Chen, C. L Yuan, K. Z. Wang, *Thin Solid Films* **2011**, *519*, 3883.

[35] a) F. Z. Wang, J. F. Fan, X. N. Dang, X. Fan, P. Wang, X. H. Wan, D. C. Zou, S. H. Kim, D. N. Lee, B. H. Kim, *J. Appl. Phys.* **2008**, *103*, 104509; b) S. D. Xun, J. D. Zhang, X. Z. Li, D.G. Ma, Z. Y. Wang, *Synth. Met.* **2008**, *158*, 484; c) H. C. Su, H.F. Chen, F.C. Fang, C.C. Liu, C.C. Wu, K.T. Wong, Y.H. Liu, S.M. Peng, *J. Am. Chem. Soc.* **2008**, 1*30*, 3413.

[36] a) W. Lu, M. C. W. Chan, N. Zhu, C. Che, C. Li, Z. Hui, *J. Am. Chem. Soc.* **2004**, *126*, 7639; b) T. Li, Y. Du, E. Wang, *Chem. Asian J.* **2008**, *3*, 1942.

[37] a) H. Y. Zhang, Z. L. Zhang, K. Q. Ye, J. Y. Zhang, Y. Wang, *Adv. Mater.* **2006**, *18*, 2369; b) M. Cölle, R. E. Dinnebier, W. Brütting, *Chem. Commun.* **2002**, 2908; c) K. Q. Ye, J. Wang, H. Sun, Y. Liu, Z. C. Mu, F. Li, S. M. Jiang, J. Y. Zhang, H. X. Zhang, Y. Wang, C. M. Che, *J. Phys. Chem. B*, **2005**, *109*, 8008; d) A. Wakamiya, T. Ide, S. Yamaguchi, *J. Am. Chem. Soc.* **2005**, *127*, 14859.

[38] H. J. Bolink, E. Coronado, R. D. Costa, N. Lardiés, E. Ortí, *Inorg. Chem.* **2008**, *47*, 9149.

[39] E. Zysman-Colman, J. D. Slinker, J. B. Parker, G. G. Malliaras, S. Bernhard, *Chem. Mater.* **2008**, *20*, 388.

[40] a) L. He, J. Qiao, L. Duan, G. F. Dong, D. Q. Zhang, L. D. Wang, Y. Qiu, *Adv. Funct. Mater.* **2009**, *19*, 2950; b) R. D. Costa, F. J. Céspedes-Guirao, E. Ortí, H. J. Bolink, J. Gierschner, F. Fernández-Lázaro, A. Sastre-Santos, *Chem. Commun.* **2009**, *26*, 3886.

[41] a) R. D. Costa, E. Ortí, H. J. Bolink, S. Graber, S. Schaffner, M. Neuburger, C. E. Housecroft, E. C. Constable, *Adv. Funct. Mater.* **2009**, *19*, 3456; b) S. Park, D. Moon, S. C. Damodharan, M. Chandran, Y. Choe, *Mater. Res. Bull.* **2012**, *47*, 2807.

[42] D. Tordera, M. Delgado, E. Ortí, H. J. Bolink, J. Frey, Md. K. Nazeeruddin, E. Baranoff, *Chem. Mater.* **2012**, *24*, 1896.

[43] a) G. Hughes, M. R. Bryce, *J. Mater. Chem.* **2005**, *15*, 94; b) H. Tokuhisa, M. Era, T. Tsutsui, *Appl. Phys. Lett.* **1998**, *72*, 2639; c) M. Strukelj, F. Papadimitrakopoulos, T. M. Miller, L. J. Rothberg, *Science* **1995**, *267*, 1969; d) S. Oyston, C. Wang, G. Hughes, A. S. Batsanov, I. F. Perepichka, M. R. Bryce, J. H. Ahn, C. Pearson, M. C. Petty, *J. Mater. Chem.* **2005**, *15*, 194.

[44] a) Y. Hamada, T. Sano, K. Shibata, K. Kuroki, *Jpn. J. Appl. Phys.* **1995**, *34*, L824; b) J. Kido, H. Shionoya, K. Nagai, *Appl. Phys. Lett.* **1995**, *67*, 2281; c) C. C. Wu, J. C. Sturm, R. A. Register, J. Tian, E. P. Dana, M. E. Thompson, *IEEE Trans. Electron Dev.* **1997**, *44*, 1269; d) C. C. Wu, J. C. Sturm, R. A. Register, M. E. Thompson, *Appl. Phys. Lett.* **1996**, *69*, 3117; e) A. R. Brown, D. D. C. Bradley, J. H. Burroughes, R. H. Friend, N. C. Greenham, P. L. Burn, A. B. Holmes, A. Kraft, *Appl. Phys. Lett.* **1992**, *61*, 2793; f) C. Adachi, S. Tokito, T. Tsutsui, S. Saito, *Jpn. J. Appl. Phys.* **1988**, *27*, L713; g) W. Huang, H. Meng, W. Yu, J. Gao, A. Heeger, *Adv. Mater.* **1998**, *10*, 593; h) W. Yu, H. Meng, J. Pei, Y.H. Lai, S.J. Chua, W. Huang, *Chem. Commun.* **1998**, 1957; i) W. Yu, H. Meng, J. Pei, W. Huang, *J. Am. Chem. Soc.* **1998**, *120*, 11808.

[45] a) K. Brunner, A. V. Dijken, H. Börner, J. J. A. M. Bastiaansen, N. M. M. Kiggen, B. M. W. Langeveld, *J. Am. Chem. Soc.* **2004**, *126*, 6035; b) W. Ma, P. K. Iyer, X. Gong, B. Liu, D. Moses, G. C. Bazan, A. J. Heeger, *Adv. Mater.* **2005**, *17*, 274; c) C. Wang, G. Y. Jung, Y. Hua, C. Pearson, M. R. Bryce, M. C. Petty, A. S. Batsanov, A. E. Goeta, J. A. K. Howard, *Chem. Mater.* **2001**, *13*, 1167; d) X. Zhan, Y. Liu, X. Wu, S. Wang, D. Zhu, *Macromolecules* **2002**, *35*, 2529; e) Y. Z. Lee, X. Chen, S. A. Chen, P. K. Wei, W. S. Fann, *J. Am. Chem. Soc.* **2001**, *123*, 2296; f) S. J. Chung, K. Y. Kwon, S. Lee, J. Jin, C. H. Lee, C. E. Lee, Y. Park, *Adv. Mater.* **1998**, *10*, 1112; g) J. H. Kim, J. H. Park, H. Lee, *Chem. Mater.* **2003**, *15*, 3414; h) W. H. Zhu, R. Yao, H. Tian, *Dyes Pigm.* **2002**, *54*, 147.

[46] a) Z. W. Xu, Y. Li, X. M. Ma, X. D. Gao, H. Tian, *Tetrahedron* **2008**, *64*, 1860; b) L. Q. Chen, C. L. Yang, J. G. Qin, *J. Organomet. Chem.* **2006**, *691*, 3519; c) W.-Y. Wong, Z. He, S.-K. So, K.-L. Tong, Z. Lin, *Organometallics* **2005**, *24*, 4079; d) Z. He, W.-Y. Wong, X. Yu, H.-S. Kwok, Z. Lin, *Inorg. Chem.* **2006**, *45*, 10922; e) Y. Zheng, A. S. Batsanov, M. R. Bryce, *Inorg. Chem.* **2011**, *50*, 3354.

[47] S. Lamansky, P. Djurovich, D. Murphy, F. Abdel-Razzaq, H. Lee, C. Adachi, P. E. Burrows, S. R. Forrest, M. E. Thompson, *J. Am. Chem. Soc.* **2001**, *123*, 4304.

[48] M. Nonoyama, *Bull. Chem. Soc. Jpn.* **1974**, *47*, 767.

[49] a) S. Sprouse, K. A. King, P. J. Spellane, R. J. Watts, *J. Am. Chem. Soc.* **1984**, *106*, 6647; b) M. G. Colombo, T. C. Brunold, T. Riedener, H. U. Güdel, M. Förtsch, H. B. Bürgi, *Inorg. Chem.* **1994**, *33*, 545.

[50] L. O. Pålsson, A. P. Monkman, *Adv. Mater.* **2002**, *14*, 757.

[51] a) S. Trasatti, *Pure Appl. Chem.* **1986**, *58*, 955; b) A. J. Bard, R. Memmimg, B. Miller, *Pure Appl. Chem.* **1991**, *63*, 569.

[52] J. V. Caspar, T. J. Meyer, *J. Phys. Chem.* **1983**, *83*, 952; b) C. Dragonetti, L. Falciola, P. Mussini, S. Righetto, D. Roberto, R. Ugo, A. Valore, *Inorg. Chem.* **2007**, *46*, 8533.

[53] a) M. A. Baldo, S. R. Forrest, *Phys. Rev. B* **2000**, *62*, 10958; b) M. A. Baldo, C. Adachi, S. R. Forrest, *Phys. Rev. B* **2000**, *62*, 10967.